

SA-DPSGD: Differentially Private Stochastic Gradient Descent based on Simulated Annealing

Jie Fu, Zhili Chen, XinPeng Ling
East China Normal University, Shanghai, China

Abstract

Differential privacy (DP) provides a formal privacy guarantee that prevents adversaries with access to machine learning models from extracting information about individual training points. Differentially private stochastic gradient descent (DPSGD) is the most popular training method with differential privacy in image recognition. However, existing DPSGD schemes lead to significant performance degradation, which prevents the application of differential privacy. In this paper, we propose a simulated annealing-based differentially private stochastic gradient descent scheme (SA-DPSGD) which accepts a candidate update with a probability that depends both on the update quality and on the number of iterations. Through this random update screening, we make the differentially private gradient descent proceed in the right direction in each iteration, and result in a more accurate model finally. In our experiments, under the same hyperparameters, our scheme achieves test accuracies 98.35%, 87.41% and 60.92% on datasets MNIST, FashionMNIST and CIFAR10, respectively, compared to the state-of-the-art result of 98.12%, 86.33% and 59.34%. Under the freely adjusted hyperparameters, our scheme achieves even higher accuracies, 98.89%, 88.50% and 64.17%. We believe that our method has a great contribution for closing the accuracy gap between private and non-private image classification.

1. Introduction

1.1. Background

In the past decade, deep learning techniques have achieved remarkable success in various machine learning/data mining tasks, like medical image recognition [7, 43, 44]. Although we do not publish the image data when training the model, hidden adversaries may steal training data information by eavesdropping and analyzing the model parameters. For example, the contents of training data can be revealed if the trained models are attacked [1, 24, 26–28], or the member information of the training dataset can be

inferred if the threat models are trained and used [2, 25]. This is of particular concern in the field of computer vision, where many applications, such as medical imaging, require the handling of sensitive and legally protected data. The EU’s General Data Privacy Regulation (GDPR) and the California Consumer Privacy Act [32] also require that machine learning practitioners need to take responsibility for protecting private data. One of the methods to prevent privacy disclosure in machine learning is the differential privacy (DP) technique [3]. The noise properly added to machine learning models published by a differentially private framework prevents unintentional leakage of private training data [4, 8, 9, 29–31].

1.2. Prior Art

Martín Abadi et al. [4] proposed the first algorithm for deep learning with differential privacy, which is named DPSGD. Subsequently, many works aimed at improving the performance of DPSGD from different aspects. On the side of adaptive DPSGD, the work of [30] used an adaptive learning rate to improve the convergence speed and reduce the privacy cost. Jaewoo Lee et al. [12] adaptively assigned different privacy budgets to each training round to mitigate the effect of noise on the gradient. Further, Zhiying Xu et al. [13] employed the Root Mean Square Prop (RMSProp) gradient descent technique to adaptively add noise to coordinates of the gradient. Zhiqi Bu et al. [15] proposed the AUTO-S clipping, which uses a small clipping norm by default and adds a positive stability constant γ in the clipping gradient direction, that eliminates the need to tune clipping norm C for any DP optimizers. For model structure, Nicolas Papernot et al. [11] founded that using a family of bounded activation functions (tempered sigmoids) instead of the unbounded activation function ReLU in DPSGD can achieve good performance. Anda Cheng et al. [41] proposed the framework that uses neural architecture search to automatically design models for private deep learning. Consequently, many works [33–35] have focused on reducing the dimensionality of the model during training to reduce the impact of noise on the overall model. Last but not least, Florian Tramet et al. [14] used Scattering Network

Table 1. This table summarizes the test accuracy of previous schemes and our scheme, SA-DPSGD, trained on the Mnist, FashionMNIST and CIFAR10 datasets. In our scheme, the values before the slash refer to the experimental results under the same hyperparameters as the previous art, and the values after the slash are the experimental results under the freely adjusted hyperparameters. For all experiments, we report the average accuracy across 5 independent runs.

Dataset	Model	(ϵ, δ)	Accuracy(%)				
			DPSGD [4]	DPSGD (tanh) [11]	DPSGD (AUTO-S) [15]	SA-DPSGD [ours]	nonDP ($\epsilon = \infty$)
Mnist	4-layer CNN	(3,1e-5)	96.73	98.05	98.12	98.35/98.89	99.09
FashionMNIST	4-layer CNN	(3,1e-5)	84.42	86.03	86.33	87.41/88.50	89.01
CIFAR10	9-layer CNN	(3,1e-5)	52.06	59.04	59.34	60.92/64.17	79.02

to traverse the image in advance to extract features before training can achieve high accuracy, but that is a pre-training method rather than a training from scratch.

The above differentially private schemes for deep learning suffer from a significant utility loss, and actually there is still an obvious accuracy gap between differentially private deep learning and non-private techniques.

1.3. Proposed Approach

Why do the existing schemes for differentially private deep learning still work not well enough? Our key observation is that in the stochastic gradient descent process these schemes allow all model updates no matter whether the corresponding objective function values get better. The fact is that in some model updates the objective function values may get worse after adding noise to gradients, especially when it is close to convergence (as shown by the blue trace line in Fig. 1). This causes two consequences: worsening the optimization objective and wasting the privacy budget. Both consequences deteriorate the resulted models.

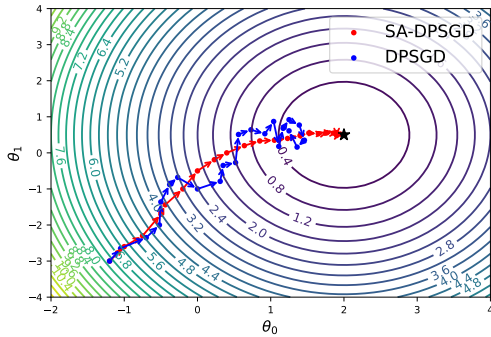


Figure 1. The simulated trajectories for DPSGD and SA-DPSGD schemes on linear regression.

Based on the key observation, our main idea of improvement is to selectively perform model updates in the differentially private stochastic gradient descent. Specifically, we accept a model update if it produces a better objective function value, and reject it with a certain probability otherwise. We use probabilistic rejections other than deterministic ones,

and, moreover, limit the number of continuous rejections, in order to avoid falling into a local optimum. This selection of model updates can make the differentially private gradient descent proceed in the right iteration, and result in a more accurate model finally (as shown by the red trace line in Fig. 1).

Our main idea can be well implemented with the simulated annealing algorithm [5]. The objective function value is the “energy”, the number of iterations is the “temperature”, a model update is a “solution”, and we reject a solution with a certain probability concerning the energy change and the temperature. Experimental results listed in Table 1 show that our scheme outperforms significantly the state-of-the-art schemes DPSGD [4], DPSGD(tanh) [11], and DPSGD(AUTO-S) [15]. When the hyperparameters are set as that used in the three schemes, our scheme achieves accuracies 98.35%, 87.41% and 60.92% on image datasets MNIST, FashionMnist and CIFAR10, respectively, compared to the best result of the three schemes, 98.12%, 86.33%, and 59.34%. When the hyperparameters are adjusted freely, our scheme achieves the best accuracies 98.89%, 88.50% and 64.17%.

1.4. Our Contribution

In summary, our contributions are follows:

- We propose an efficient scheme, SA-DPSGD, for differentially private deep learning, using the simulated annealing algorithm to select model updates with probability during the stochastic gradient descent process.
- We theoretically prove that SA-DPSGD satisfies differential privacy, and analyze its privacy loss with respect to the method of Rényi Differential Privacy (RDP).
- We fully implement the SA-DPSGD, and conduct extensive experiments on various datasets to demonstrate that it outperforms the state-of-the-art schemes significantly.

2. Preliminary Knowledge

In this section, we briefly introduce the definition of differential privacy, the differentially private stochastic gradient descent (DPSGD) algorithm, and the simulated annealing algorithm.

2.1. Differential Privacy

Differential privacy is a rigorous mathematical framework that formally defines data privacy. Informally, it states that changes to a single data point in the input dataset cannot result in statistically significant changes in the output [3, 37, 38] if differential privacy holds.

Definition 1 (Differential Privacy [3]). *The randomized mechanism A provides (ϵ, δ) -Differential Privacy (DP), if for any two neighboring database D and D' that differ in only a single entry, $\forall S \subseteq \text{Range}(A)$,*

$$\Pr(A(D) \in S) < e^\epsilon \Pr(A(D') \in S) + \delta \quad (1)$$

Here, $\epsilon > 0$ gives the level of privacy guarantee in the worst case. The smaller ϵ is, the higher the privacy level is. The factor $\delta > 0$ allows for some probability that the property does not hold. In practice, this δ is required to be very small, and generally smaller than $1/|D|$.

There are many attractive properties of DP. Sequential composition of DP will smoothly degrade privacy budget with multiple accesses to the same data. In addition, the output of a differentially private algorithm, can be arbitrarily processed without compromising the privacy guarantees, which is called the post-processing property.

2.2. DPSGD

Differentially Private Stochastic Gradient Descent (DPSGD), which was introduced by Abadi et al. [4], is the first scheme for training deep neural networks with differential privacy guarantees. DPSGD adds noise to gradients in the training process, and results in models with differential privacy. Specifically, it clips each per-sample gradient according to a fixed ℓ_2 norm, and adds Gaussian noise scaling with this norm to the sum of the gradients when computing the batch-averaged gradients. Then, the gradient descent is performed based on the batch-averaged gradients. Since initial models are randomly generated and independent on the sample data, and the batch-averaged gradients satisfy the differential privacy, the resulted models also satisfy the differential privacy due to the post-processing property.

Originally, DPSGD employs moments accountant approach to calculate the privacy loss. In this work, for fair comparison, we all use the Rényi differential privacy (RDP) approach [6, 21] instead for privacy accountant. RDP is a generalization of differential privacy that uses the α -Rényi divergences, and the RDP approach is implemented in Opacus [19] and Tensorflow Privacy [42].

2.3. Simulated Annealing Algorithm

Simulated Annealing (SA) algorithm is a heuristic optimization algorithm proposed by Metropolis et al. [45]. The idea of the algorithm was inspired by the physical annealing process, where when an object is cooled down, the probability of finding a low-energy particle increases gradually.

In the context of optimization, Kirkpatrick et al. [5] regarded objective function value as the energy, and finding a better solution as finding a lower-energy particle. Assuming the objective function of the problem is $f(x)$, the current temperature is T_i , the current feasible solution is x_i , and the new solution is x' , according to the simulated annealing process, the probability that the new solution x' is accepted as the next feasible solution x_{i+1} is designed as Eq. (2), and the simulated annealing algorithm is depicted in Algorithm 1.

$$P(x' \rightarrow x_{i+1}) = \begin{cases} 1, & f(x') \leq f(x_i) \\ e^{-\frac{f(x') - f(x_i)}{T_i}}, & f(x') > f(x_i) \end{cases} \quad (2)$$

Algorithm 1 Simulated Annealing Algorithm

Input: Objective function f to be minimized, initial temperature $T_0 > 0$, cooling factor $\alpha \in (0, 1)$, number of iterations n

- 1: Initialize: initial solution $s^{(0)}$, $T = T_0$
 - 2: **for** $i = 0, \dots, n - 1$ **do**
 - 3: Pick a new solution s_{new} in a neighborhood of $s^{(i)}$
 - 4: $\Delta f = f(s_{new}) - f(s^{(i)})$
 - 5: $prob = e^{-\Delta f/T}$
 - 6: **if** $\text{random}(0, 1) < prob$ **then**
 - 7: $s^{(i+1)} = s_{new}$
 - 8: **else**
 - 9: $s^{(i+1)} = s^{(i)}$
 - 10: **end if**
 - 11: $T = \alpha \cdot T$
 - 12: **end for**
 - 13: **Output** the last solution $s^{(n-1)}$
-

3. SA-DPSGD

In this section, we first give the overview of SA-DPSGD, then describe its detailed design, and finally provide the privacy analysis.

3.1. Overview

We combine our main idea of selecting model updates with the simulated annealing algorithm, and design the SA-DPSGD scheme. The high-level description of our scheme is as follows.

- We generate new solutions (updates) iteratively by DPSGD, and compute the energy (objective function

value) accordingly. The acceptance probability of the current solution is then determined by the energy change from the previous iteration to the current one, and the number of accepted solutions by far. Note that we use the number of accepted solutions instead of that of all generated solutions to more accurately reflect the effectiveness of actual iterations.

- We let the acceptance probability be always 1, when the energy change is negative. That is, we always accept the solutions (updates) that step in the right direction. Even though our model updates are noisy, which means that the actual energy may be positive with a tiny probability, this still guarantees that the training proceeds mainly in the direction to convergence.
- We let the acceptance probability decreases exponentially as the energy change and the number of accepted solutions increase, when the energy change is positive. In this case, the energy would become worse if a solution were accepted. However, deterministic rejections may cause the final solution to fall in a local optimum. Therefore, we accept solutions of positive energy changes with a small, decreasing probability.
- We limit the number of continuous rejections, and accept a solution anyway if too many successive rejections take place previously. When the training is close to convergence, the acceptance probability may become so small that it nearly rejects all solutions with positive energy changes, and may reach a local optimum. Limitation of the continuous rejections avoids this problem by accepting a solution anyway when necessary.

Following the above high-level description, we depict the work flow of SA-DPSGD as shown in Fig. 2. First, all the parameters are initialized. Given the initial temperature Q_0 , the rejection threshold μ_0 , and the total number of iterations T , the number of iterations t , the number of accepted solutions τ , and the number of rejections μ are all set to 0, and the initial model w_0 is randomly generated. Next, we use the cross-entropy loss function as the objective function, and in the current iteration (assuming the $(t + 1)$ -th iteration), a new solution w_{new} , its energy $J(w_{new})$, and the energy change ΔE from the previous iteration to the current one, are computed using DPSGD. Then, the neural network determines whether to accept the new solution. If the number of continuous rejections μ exceeds the threshold value μ_0 , it accepts the solution anyway, i.e., $w_{t+1} = w_{new}$; otherwise, it accepts the solution with a probability P as Eq. (3), where Q is the current temperature.

$$P = \begin{cases} 1, & \Delta E \leq 0 \\ e^{-\Delta E * Q}, & \Delta E > 0 \end{cases} \quad (3)$$

Note that, SA-DPSGD differs from conventional simulated annealing algorithm in the definition of temperature. We define the temperature $Q = Q_0 \cdot \tau$, where Q_0 is the initial temperature and τ is the number of accepted solutions by far. Therefore, our temperature increases instead as the training proceeds. However, we compute the acceptance probability by multiplying instead of dividing the temperature. This makes the probability decrease as the training goes, which is just the same as the conventional simulated annealing algorithm.

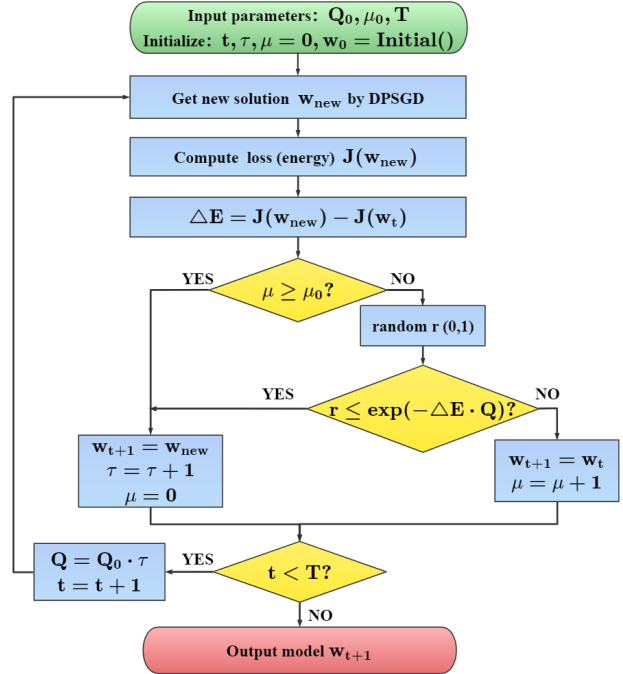


Figure 2. The work flow of SA-DPSGD.

3.2. Detailed Design

We now present the detailed design of SA-DPSGD in Algorithm 2, which consists of the following steps.

- **Step0: Initialization (Line 1).** Initialize parameters (μ_0, Q_0, w_0 , etc.)
- **Step1: Gradient Computation (Lines 3 and 5).** Randomly select a small batch of samples B_t from the training dataset, and for each sample $i \in B_t$, calculate the corresponding gradient values.
- **Step2: Gradient Clipping (Line 6).** Clip the gradients of each sample so that the l_2 norm of the gradients is not greater than the clipping norm C .
- **Step3: Noise Adding (Line 8).** First sum the clipped gradients, then add Gaussian noise $\mathcal{N}(0, C^2 \sigma^2)$ to the sum, and finally compute the average.

- **Step4: Gradient Decent (Line 9).** Perform gradient descent using the noisy gradients to obtain a new solution (model update) w_{new} for the current iteration.
- **Step5: Evaluating New Solution (Lines 11 to 20).** Compute the energy (i.e., objective function value) $J(w_{new})$ of the new solution, and subtract the energy of the previous iteration from it to get the energy change ΔE . The new solution is accepted if the number of rejections exceeds the rejection threshold, i.e., $\mu \geq \mu_0$; otherwise, it is accepted with a probability P base on Eq. (3).
- **Step6: Raising the temperature (Lines 22).** We let the current temperature $Q = Q_0 \cdot \tau$, so that the temperature rises periodically to produce a lower acceptance probability as the training proceeds.
- Repeat steps 1-6 until the threshold T for the total number of training sessions is reached. Finally, the model w_{t+1} is output and the privacy loss is calculated according to Theorem 1.

3.3. Privacy Analysis

In SA-DPSGD as shown in Algorithm 2, initial models are randomly generated not depending on sample data, the batch-averaged gradients are added noise to satisfy differential privacy, and all other operations including model selecting and model updating are only based on the initial models and the batch-averaged gradients. Thus, SA-DPSGD satisfies differential privacy due to the post-processing property.

We claim that the privacy loss caused by SA-DPSGD is only dependent on the number of accepted model updates τ , since when final models are published, only the results of accepted model updates can be seen, and whether resampling batches and re-generating noise are simply unknown. Theorem 1 shows the privacy loss calculation of SA-DPSGD.

Theorem 1 (*DP Privacy Loss of SA-DPSGD*). *After τ iterations of model gradient decent, the privacy loss of SA-DPSGD satisfies:*

$$(\epsilon, \delta) = \left(\frac{\tau}{\alpha - 1} \sum_{i=0}^{\alpha} \binom{\alpha}{i} (1 - q)^{\alpha - i} q^i \exp\left(\frac{i^2 - i}{2\sigma^2}\right) + \frac{\log 1/\delta}{\alpha - 1}, \delta \right) \quad (4)$$

where $q = \frac{B}{N}$, σ is noise scale, and $\alpha > 1$ is the order.

Proof. We calculate the privacy loss based on RDP approach [6]. We first use the sampling Gaussian theorem of RDP to calculate the privacy cost of each iteration, then

Algorithm 2 SA-DPSGD

Input: Samples $\{x_1, \dots, x_N\}$, loss function $\mathcal{L}(\theta, x)$. Parameters: total number of iterations T , learning rate η , noise scale σ , batch size B , clipping norm C , rejection threshold μ_0 , initial temperature Q_0

- 1: Initialize: $t, \tau, \mu = 0, Q = Q_0, w_0$
- 2: **while** $t < T$ **do**
- 3: Sample randomly a batch B_t with probability B/N
- 4: **for** $i \in B_t$ **do**
- 5: Compute $g_t(x_i) \leftarrow \nabla \mathcal{L}(w_t, x_i)$
- 6: $\bar{g}_t(x_i) \leftarrow g_t(x_i) / \max(1, \frac{\|g_t(x_i)\|_2}{C})$
- 7: **end for**
- 8: $\tilde{g}_t \leftarrow \frac{1}{B} (\sum_i^{B_t} \bar{g}_t(x_i) + \mathcal{N}(0, \sigma^2 C^2))$
- 9: $w_{new} = w_t - \eta_t \tilde{g}_t$
- 10: Compute test loss $J(w_{new})$
- 11: $\Delta E = J(w_{new}) - J(w_t)$
- 12: $P = e^{-\Delta E \cdot Q}$
- 13: **if** $\text{random}(0, 1) \leq P$ **or** $\mu \geq \mu_0$ **then**
- 14: $w_{t+1} = w_{new}$
- 15: $\tau = \tau + 1$
- 16: $\mu = 0$
- 17: **else**
- 18: $w_{t+1} = w_t$
- 19: $\mu = \mu + 1$
- 20: **end if**
- 21: $t = t + 1$
- 22: $Q = Q_0 \cdot \tau$
- 23: **end while**
- 24: Compute privacy loss (ϵ, δ) by Theorem 1
- 25: **Output** w_{t+1} and privacy loss (ϵ, δ)

use the composition of RDP mechanisms to compute the privacy cost of multiple iterations, and finally convert the obtained RDP cost to DP cost.

Definitions 2 and 3 define Sampled Gaussian Mechanism (SGM) and Rényi Differential Privacy (RDP), respectively.

Definition 2 (*Sampled Gaussian Mechanism (SGM) [21]*). *Let f be a function mapping subsets of S to \mathbb{R}^d . We define the Sampled Gaussian Mechanism (SGM) parameterized with the sampling rate $0 < q \leq 1$ and the $\sigma > 0$ as*

$$SG_{q, \sigma}(S) \triangleq f(\{x : x \in S \text{ is sampled with probability } q\}) + \mathcal{N}(0, \sigma^2 \mathbb{I}^d) \quad (5)$$

in SA-DPSGD, f is the clipped gradient evaluation on sampled data points $f(\{x_i\}_{i \in B}) = \sum_{i \in B} \bar{g}_t(x_i)$. If \bar{g}_t is obtained by clipping g_t with a gradient norm bound C , then the sensitivity of f is equal to C .

Definition 3 (*RDP privacy budget of SGM [21]*). *Let $SG_{q, \sigma}$, be the Sampled Gaussian Mechanism for some func-*

tion f . If f has sensitivity 1, $SG_{q,\sigma}$ satisfies (α, ϵ) -RDP whenever

$$\epsilon \leq \frac{1}{\alpha - 1} \log \max(A_\alpha(q, \sigma), B_\alpha(q, \sigma)) \quad (6)$$

where

$$\begin{cases} A_\alpha(q, \sigma) \triangleq \mathbb{E}_{z \sim \mu_0} [(\mu(z)/\mu_0(z))^\alpha] \\ B_\alpha(q, \sigma) \triangleq \mathbb{E}_{z \sim \mu} [(\mu_0(z)/\mu(z))^\alpha] \end{cases} \quad (7)$$

with $\mu_0 \triangleq \mathcal{N}(0, \sigma^2)$, $\mu_1 \triangleq \mathcal{N}(1, \sigma^2)$ and $\mu \triangleq (1 - q)\mu_0 + q\mu_1$.

Furthermore, it holds $\forall (q, \sigma) \in (0, 1] \times \mathbb{R}^+$, $A_\alpha(q, \sigma) \geq B_\alpha(q, \sigma)$. Thus, $SG_{q,\sigma}$ satisfies $(\alpha, \frac{1}{\alpha-1} \log(A_\alpha(q, \sigma)))$ -RDP.

Finally, paper [21] describes a procedure to compute $A_\alpha(q, \sigma)$ depending on integer α as Eq. (8).

$$A_\alpha = \sum_{k=0}^{\alpha} \binom{\alpha}{k} (1-q)^{\alpha-k} q^k \exp\left(\frac{k^2 - k}{2\sigma^2}\right) \quad (8)$$

Lemma 1 gives the composition of RDP mechanisms.

Lemma 1 (Composition of RDP [6]). For two randomized mechanisms f, g such that f is (α, ϵ_1) -RDP and g is (α, ϵ_2) -RDP the composition of f and g which is defined as (X, Y) (a sequence of results), where $X \sim f$ and $Y \sim g$, satisfies $(\alpha, \epsilon_1 + \epsilon_2)$ -RDP

According to Definitions 2 and 3, and Lemma 1, we have Theorem 2.

Theorem 2 Given the sampling rate $q = \frac{B}{N}$ for each iteration of the local dataset and the noise factor σ for all iterations, the total RDP privacy loss for T accepted iterations for any integer $\alpha \geq 2$ is given in Eq (9).

$$\epsilon'(\alpha)_T = \frac{T}{\alpha - 1} \sum_{i=0}^{\alpha} \binom{\alpha}{i} (1-q)^{\alpha-i} q^i \exp\left(\frac{i^2 - i}{2\sigma^2}\right) \quad (9)$$

Lemmas 2 and 3 give two ways of conversion from RDP to DP, and the latter is more compact. However, since the previous work used Lemma 2 for calculating privacy loss, for fair comparison we also uses it in this work.

Lemma 2 (Conversion from RDP to DP [6]). If a randomized mechanism $f : D \rightarrow \mathbb{R}$ satisfies (α, ϵ) -RDP, then it satisfies $(\epsilon + \frac{\log 1/\delta}{\alpha-1}, \delta)$ -DP where $0 < \delta < 1$

Lemma 3 (Better conversion from RDP to DP [36]). If a mechanism M is (α, ϵ) -RDP, then it is $(\epsilon + \log((\alpha-1)/\alpha) - (\log \delta + \log \alpha)/(\alpha-1), \delta)$ for any $0 < \delta < 1$.

By Theorem 2 and Lemma 2, Theorem 1 is proved. \square

In practice, given σ , δ and B at each iteration, we select α from $\{2, 3, \dots, 64\}$ and determine the smallest ϵ_* in Theorem 1. The privacy loss is the pair (ϵ_*, δ) .

4. Experiment

We evaluate SA-DPSGD on three datasets: MNIST, FashionMNIST and CIFAR10. Although the three datasets are regarded as “solved” in the computer vision community [39, 40], they still remain challenging in the context of differential privacy [10, 19, 22].

4.1. Initialization

Dataset. MNIST [16] is the standard dataset for handwritten digit recognition and FashionMNIST [17] is the dataset for clothing classification, both of them consist of 60,000 training examples and 10,000 testing examples. Each example is a 28×28 gray-level image. CIFAR10 [18] consists of color images classified into 10 classes, and partitioned into 50,000 training examples and 10,000 test examples. Each example is a 32×32 image with three channels (RGB).

Network model. For MNIST and FashionMNIST, we use a simple convolutional neural network with 4 layers, and for CIFAR10, we use a deeper convolutional neural network model with 9 layers. The network architectures are all the same as previous work [11, 14, 15].

Parameter settings. Our experiments are implemented with SGD optimizer by pytorch [23]. All hyperparameter settings for this experiment, detailed in Table 2, are the same as [14, 15], except the initial temperature Q_0 and rejection threshold μ_0 are new parameters in our scheme.

Table 2. The setting of hyperparameters

Parameter	MNIST	Fashion MNIST	CIFA R10
Learning rate η	0.5	4.0	1.0
Batch size B	512	2048	1024
Clipping norm C	0.1	0.1	0.1
Noise scale σ	1.23	2.15	1.54
Privacy budget (ϵ, δ)	(3,1e-5)	(3,1e-5)	(3,1e-5)
Initial temperature Q_0	10.0	10.0	10.0
Rejection threshold μ_0	10	10	5

Baselines and prior state-of-the-art. We evaluate the privacy cost and accuracy of our approach SA-DPSGD compared with state-of-the-art schemes: DPSGD [4], DPSGD(tanh) [11] and DPSGD(AUTO-S) [15]. They are all differentially private deep learning schemes from scratch, where DPSGD uses ReLU as the activation function of the neural network by default, DPSGD(tanh) and DPSGD(AUTO-S) apply tanh activation function instead. To the best of our knowledge, DPSGD(AUTO-S) performs best among the existing differentially private deep learning methods from scratch. Our scheme selects tanh as the activation function, and all schemes apply the above network

structure and parameter settings.

4.2. Privacy Cost

We compare the privacy cost of our scheme, SA-DPSGD, with that of the state-of-the-art schemes, when achieving the same accuracy on datasets MNIST, FashionMNIST and CIFAR10. The experimental results are summarized in Table 3, where ϵ_D , ϵ_H , ϵ_A and ϵ_S denote the minimum privacy cost of DPSGD, DPSGD(tanh), DPSGD(AUTO-S) and SA-DPSGD, respectively. The parameter δ is set to 10^{-5} , and RDP approach is used for privacy loss calculation for all the schemes. We observe that SA-DPSGD always has a lower privacy cost than other schemes, and the higher the privacy costs are, the bigger the gap of privacy costs is. The reason should be that our scheme accepts right model updates, and rejects wrong ones, which speeds up the convergence while saves the privacy cost, and when the privacy costs are higher, the saving is more obvious.

Table 3. This table summarizes the privacy cost of previous works and our scheme SA-DPSGD trained on datasets MNIST, FashionMNIST and CIFAR10 when a pre-specified level of test accuracy was achieved. For all experiments, we report the average privacy loss across 5 independent runs. "-" indicates that the corresponding accuracy cannot be achieved within $\epsilon \leq 6$.

Dataset	Accuracy	ϵ_D	ϵ_H	ϵ_A	ϵ_S
MNIST	0.94	1.64	1.23	1.22	1.21
	0.96	2.47	1.47	1.47	1.46
	0.98	-	2.92	2.91	2.53
Fashion MNIST	0.82	2.20	1.73	1.64	1.52
	0.84	2.88	2.08	2.07	1.86
	0.86	5.86	2.96	2.92	2.51
CIFAR10	0.52	2.99	2.15	2.05	1.93
	0.55	3.68	2.39	2.36	2.27
	0.58	4.54	2.83	2.80	2.57

4.3. Performace

We compare the utility of the four schemes when achieving the same privacy level. Fig. 3 shows the privacy-utility Pareto curves [20] for the DPSGD, DPSGD(tanh), DPSGD(AUTO-S) and SA-DPSGD trained on all three datasets. Fig. 3(a-c) shows the test loss and privacy loss curves, we can see that SA-DPSGD almost always outperforms the previous schemes in terms of loss values. Fig. 3(d-f) shows the accuracy and privacy loss curves, and again, SA-DPSGD almost always outperforms other schemes. In particular, we can see that the larger the privacy budget is, the better SA-DPSGD outperforms the previous schemes. The reason is that our scheme selects model

updates that are beneficial to model convergence by simulated annealing. This allows the model to further approach convergence in the late iterations and also saves the privacy budget. The previous schemes cannot avoid the effect from random noise, so they are difficult to further converge in the late iterations.

Table 1 summarizes the results with hyperparameters provided in previous work for each of the three datasets considered in our experiments. In their own best settings and network model, the SA-DPSGD continues to consistently outperform the state-of-the-art schemes [4, 11, 15]. For a privacy guarantee of $(\epsilon, \delta) = (3, 10^{-5})$, compared to DPSGD(AUTO-S) [15] which is currently the best scheme to our knowledge, our scheme achieves a test accuracy of 98.35% on MNIST (instead of 98.12%), 87.41% on FashionMNIST (instead of 86.33%), and 60.92% on CIFAR10 (instead of 59.34%). Furthermore, if we select hyperparameters freely, our scheme can reach even higher accuracies 98.89%, 88.50% and 64.17% in the above three datasets.

4.4. Impact of Parameters

In this set of experiments, we study the impact of the learning rate, the batch size, the initial temperature and the rejection threshold on the MNIST dataset. In all experiments, if not specified, we use the SGD optimizer, and set the learning rate $\eta = 0.5$, batch size $B = 512$, initial temperature $Q_0 = 10$, rejection threshold $\mu_0 = 10$, noise scale $\sigma = 1.23$, and privacy budget of $(3, 1e - 5)$.

Learning Rate. As shown in Fig. 4a, the test accuracy stays consistently above 96.5%, irrespective of the learning rate ranging from 0.1 to 2.0. When the learning rate is lower than 1.5, the accuracy increases with the learning rate. When it is higher than 1.5, a higher learning rate results in a lower accuracy. In particular, when our method is set to a learning rate of 1.5, the test accuracy can reach 98.81%.

Batch Size. The batch size impacts on the sampling ratio, a large batch size yields a higher sampling ratio and reduces the number of training steps. A small batch size will lead to more Gaussian noise effects so that making the model fail to converge. Fig. 4b depicts the accuracy versus batch size. It can be observed that as the batch size grows, the performance (test accuracy reach 98.89%) peaks at batch size equal to 256, and finally declines.

Initial Temperature. The initial temperature Q_0 determines the probability of accepting an inferior solution each time, and the larger the initial temperature is, the less likely it is to accept an inferior solution. But too high an initial temperature will often put the model into a saddle point. From the Fig. 4c, we can see that when $Q_0 > 1$, the accuracy does not decrease and the difference is not significant.

Rejection Threshold. The rejection threshold μ_0 indicates the number of times our algorithm can continuously reject inferior solutions. A higher rejection threshold means

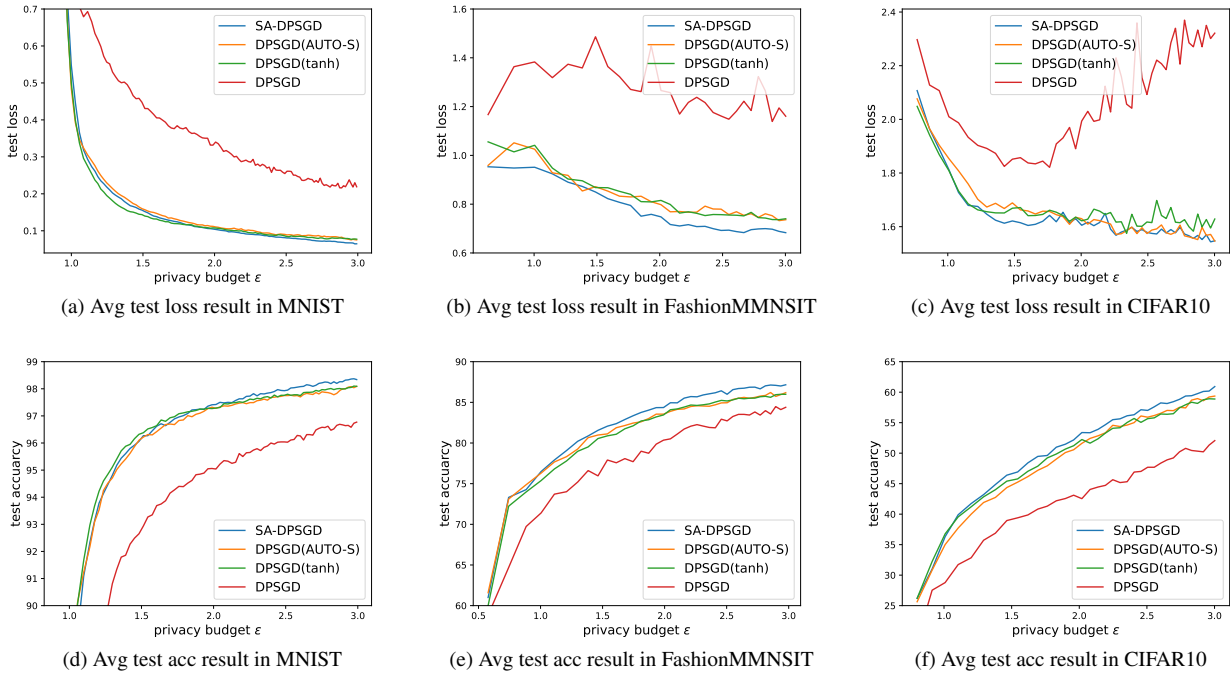


Figure 3. Test average loss and accuracy as a function of the privacy loss when training with SA-DPSGD, DPSGD(AUTO-S), DPSGD(tanh) and DPSGD on MNIST, FashionMNIST, and CIFAR10 (left to right). All elements of the architecture (number, type, and dimension of layers) and the hyperparameters (learning rate, batch size, clipping norm and noise scale) are identical. Results averaged over 5 runs.

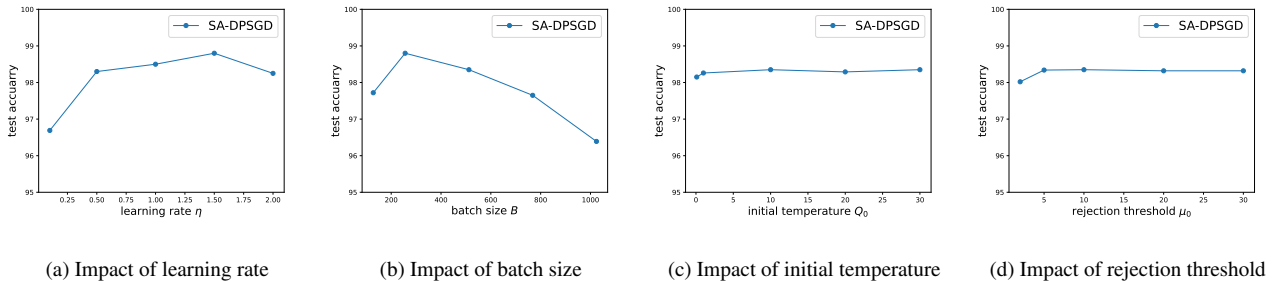


Figure 4. The impact of different parameters on the test accuracy of SA-DPSGD.

more consecutive rejections of inferior solutions, and vice versa. Fig. 4d shows that the relation of performance and rejection threshold μ_0 . After μ_0 reaches 5, the accuracy rate remains basically the same. So a high μ_0 does not help us to get higher accuracy, but on the contrary, it increases the training time.

5. CONCLUSION

We have proposed a differentially private scheme for stochastic gradient descent based on simulated annealing, SA-DPSGD. Our scheme uses the idea of simulated annealing to select right model updates that facilitate the convergence during the iterations. This saves the cost of privacy

budget, and finally results in more accurate models. Extensive experiments have shown that our scheme outperforms significantly the state-of-the-art schemes, DPSGD, DPSGD(tanh) and DPSGD(AUTO-S) in term of privacy cost or test accuracy. At the same time, our scheme is widely applicable and can be applied to any dataset and any neural network structure. It can serve as a strong canonical baseline for evaluating proposed improvements over DPSGD in the future. However, our scheme is time-consuming, and the future work is to investigate the choice of newly introduced hyperparameters in SA-DPSGD to trade off test accuracy and computation time.

References

- [1] L. Zhu, Z. Liu, and S. Han, “Deep leakage from gradients,” *Advances in Neural Information Processing Systems*, vol. 32, 2019. 1
- [2] C. Song, T. Ristenpart, and V. Shmatikov, “Machine learning models that remember too much,” pp. 587–601, 2017. 1
- [3] C. Dwork, A. Roth *et al.*, “The algorithmic foundations of differential privacy,” *Foundations and Trends® in Theoretical Computer Science*, vol. 9, no. 3–4, pp. 211–407, 2014. 1, 3
- [4] M. Abadi, A. Chu, I. Goodfellow, H. B. McMahan, I. Mironov, K. Talwar, and L. Zhang, “Deep learning with differential privacy,” *Computer and Communications Security*, 2016. 1, 2, 3, 6, 7
- [5] S. Kirkpatrick, C. D. Gelatt, and M. P. Vecchi, “Optimization by simulated annealing,” *Science*, 1983. 2, 3
- [6] I. Mironov, “Rényi differential privacy,” *IEEE Computer Security Foundations Symposium*, 2017. 3, 5, 6
- [7] A. Lundervold and A. Lundervold, “An overview of deep learning in medical imaging focusing on mri,” *Zeitschrift Fur Medizinische Physik*, 2018. 1
- [8] N. Carlini, C. Liu, Ú. Erlingsson, J. Kos, and D. Song, “The secret sharer: Evaluating and testing unintended memorization in neural networks,” *Usenix Security Symposium*, 2019. 1
- [9] V. Feldman, “Does learning require memorization? a short tale about a long tail,” *Symposium on The Theory of Computing*, 2019. 1
- [10] E. Bagdasaryan, O. Poursaeed, and V. Shmatikov, “Differential privacy has disparate impact on model accuracy,” *Neural Information Processing Systems*, 2019. 6
- [11] N. Papernot, A. Thakurta, S. Song, S. Chien, and Ú. Erlingsson, “Tempered sigmoid activations for deep learning with differential privacy,” *National Conference on Artificial Intelligence*, 2020. 1, 2, 6, 7
- [12] J. Lee and D. Kifer, “Concentrated differentially private gradient descent with adaptive per-iteration privacy budget,” *Knowledge Discovery and Data Mining*, 2018. 1
- [13] Z. Xu, S. Shi, A. X. Liu, J. Zhao, and L. Chen, “An adaptive and fast convergent approach to differentially private deep learning,” *International Conference on Computer Communications*, 2019. 1
- [14] F. Tramèr and D. Boneh, “Differentially private learning needs better features (or much more data),” *Learning*, 2020. 1, 6
- [15] Z. Bu, Y.-X. Wang, S. Zha, and G. Karypis, “Automatic clipping: Differentially private deep learning made easier and stronger,” 2022. 1, 2, 6, 7
- [16] L. Deng, “The mnist database of handwritten digit images for machine learning research,” *IEEE Signal Processing Magazine*, 2012. 6
- [17] H. Xiao, K. Rasul, and R. Vollgraf, “Fashion-mnist: a novel image dataset for benchmarking machine learning algorithms,” *arXiv: Learning*, 2017. 6
- [18] A. Krizhevsky, “Learning multiple layers of features from tiny images,” 2009. 6
- [19] A. Yousefpour, I. Shilov, A. Sablayrolles, D. Testuggine, K. Prasad, M. Malek, J. Nguyen, S. Ghosh, A. Bharadwaj, J. Zhao, G. Cormode, and I. Mironov, “Opacus: User-friendly differential privacy library in pytorch,” *arXiv: Learning*, 2021. 3, 6
- [20] B. Avent, J. González, T. Diethe, A. Paleyes, and B. Balle, “Automatic discovery of privacy-utility pareto fronts,” *arXiv: Machine Learning*, 2019. 7
- [21] I. Mironov, K. Talwar, and L. Zhang, “Rényi differential privacy of the sampled gaussian mechanism,” *arXiv: Learning*, 2019. 3, 5, 6
- [22] N. Papernot, “Machine learning at scale with differential privacy in {TensorFlow},” in *2019 {USENIX} Conference on Privacy Engineering Practice and Respect ({PEPR} 19)*, 2019. 6
- [23] A. D. I. Pytorch, “Pytorch,” 2018. 6
- [24] Z. Wang, M. Song, Z. Zhang, Y. Song, Q. Wang, and H. Qi, “Beyond inferring class representatives: User-level privacy leakage from federated learning,” *International Conference on Computer Communications*, 2018. 1
- [25] L. Melis, C. Song, E. D. Cristofaro, and V. Shmatikov, “Exploiting unintended feature leakage in collaborative learning,” *IEEE Symposium on Security and Privacy*, 2022. 1

- [26] L. T. Phong, Y. Aono, T. Hayashi, L. Wang, and S. Moriai, "Privacy-preserving deep learning: Revisited and enhanced," *International Conference on Applications and Techniques in Information Security*, 2017. 1
- [27] M. Nasr, R. Shokri, and A. Houmansadr, "Comprehensive privacy analysis of deep learning: Passive and active white-box inference attacks against centralized and federated learning," *arXiv: Machine Learning*, 2018. 1
- [28] M. Fredrikson, S. Jha, and T. Ristenpart, "Model inversion attacks that exploit confidence information and basic countermeasures," *Computer and Communications Security*, 2015. 1
- [29] R. Shokri and V. Shmatikov, "Privacy-preserving deep learning," *Allerton Conference on Communication, Control, and Computing*, 2015. 1
- [30] A. Koskela and A. Honkela, "Learning rate adaptation for differentially private stochastic gradient descent," 2018. 1
- [31] L. Xiang, J. Yang, and B. Li, "Differentially-private deep learning from an optimization perspective," *International Conference on Computer Communications*, 2019. 1
- [32] R. Cummings and D. Desai, "The role of differential privacy in gdpr compliance," in *FAT'18: Proceedings of the Conference on Fairness, Accountability, and Transparency*, 2018. 1
- [33] A. Golatkar, A. Achille, Y.-X. Wang, A. Roth, M. Kearns, and S. Soatto, "Mixed differential privacy in computer vision," 2022. 1
- [34] D. Yu, H. Zhang, W. Chen, and T.-Y. Liu, "Do not let privacy overbill utility: Gradient embedding perturbation for private learning," *Learning*, 2021. 1
- [35] Y. Zhou, Z. S. Wu, and A. Banerjee, "Bypassing the ambient dimension: Private sgd with gradient subspace identification," *Learning*, 2020. 1
- [36] B. Balle, G. Barthe, M. Gaboardi, J. Hsu, and T. Sato, "Hypothesis testing interpretations and renyi differential privacy," in *International Conference on Artificial Intelligence and Statistics*. PMLR, 2020, pp. 2496–2506. 6
- [37] C. Dwork, F. McSherry, K. Nissim, and A. Smith, "Calibrating noise to sensitivity in private data analysis," *Lecture Notes in Computer Science*, 2006. 3
- [38] C. Dwork, "A firm foundation for private data analysis," *Communications of The ACM*, 2011. 3
- [39] K. He, X. Zhang, S. Ren, and J. Sun, "Deep residual learning for image recognition," *arXiv: Computer Vision and Pattern Recognition*, 2015. 6
- [40] G. Huang, Z. Liu, L. van der Maaten, and K. Q. Weinberger, "Densely connected convolutional networks," *Computer Vision and Pattern Recognition*, 2016. 6
- [41] A. Cheng, J. Wang, X. S. Zhang, Q. Chen, P. Wang, and J. Cheng, "Dpnas: Neural architecture search for deep learning with differential privacy," *national conference on artificial intelligence*, 2021. 1
- [42] Google, "Tensorflow privacy," <https://github.com/tensorflow/privacy>, 2018. 3
- [43] S. K. Zhou, H. Greenspan, C. Davatzikos, J. S. Duncan, B. van Ginneken, A. Madabhushi, J. L. Prince, D. Rueckert, and R. M. Summers, "A review of deep learning in medical imaging: Imaging traits, technology trends, case studies with progress highlights, and future promises," *arXiv: Computer Vision and Pattern Recognition*, 2020. 1
- [44] A. J. Anaya-Isaza, L. Mera-Jiménez, and M. Zequera-Diaz, "An overview of deep learning in medical imaging," *Informatics in Medicine Unlocked*, 2021. 1
- [45] N. Metropolis, A. W. Rosenbluth, M. N. Rosenbluth, A. H. Teller, and E. Teller, "Equation of state calculations by fast computing machines," *Journal of Chemical Physics*, 1953. 3